

Exceptional points of Bloch eigenmodes on a dielectric slab with a periodic array of cylinders

Amgad Abdrabou* and Ya Yan Lu

Department of Mathematics, City University of Hong Kong, Kowloon, Hong Kong, China

(Dated: April 7, 2020)

Eigenvalue problems for electromagnetic resonant states on open dielectric structures are non-Hermitian and may have exceptional points (EPs) at which two or more eigenfrequencies and the corresponding eigenfunctions coalesce. EPs of resonant states for photonic structures give rise to a number of unusual wave phenomena and have potentially important applications. It is relatively easy to find a few EPs for a structure with parameters, but isolated EPs provide no information about their formation and variation in parameter space, and it is always difficult to ensure that all EPs in a domain of the parameter space are found. In this paper, we analyze EPs for a dielectric slab containing a periodic array of circular cylinders. By tuning the periodic structure towards a uniform slab and following the EPs continuously, we are able to obtain a precise condition about the limiting uniform slab, and thereby order and classify EPs as tracks with their endpoints determined analytically. It is found that along each track, a second order EP of resonant states (with a complex frequency) is transformed to a special kind of third order EP with a real frequency via a special fourth order EP. Our study provides a clear and complete picture for EPs in parameter space, and gives useful guidance to their practical applications.

I. INTRODUCTION

A non-Hermitian eigenvalue problem (EVP) often has multiple eigenvalues sharing a single linearly independent eigenfunction. For EVPs depending on parameters, the set of parameter values corresponding to such a non-Hermitian degeneracy is called an exceptional point (EP)[1–3]. In the photonics community, there is currently a significant research effort to construct systems with EPs, find their unusual properties, and realize their applications [4, 5]. The associated EVPs are either directly formulated from the governing Maxwell’s equations or indirectly formulated from the scattering operators. For parity-time (\mathcal{PT}) symmetric photonic systems [5–7], EPs can be easily found by tuning a single parameter, namely, the magnitude of the the balanced gain and loss. A number of interesting wave phenomena have been observed in photonic systems with \mathcal{PT} symmetry and EPs [8, 9]. Potential applications of EPs include lasing [10, 11], sensing [12–16], robust mode switching [17, 18], etc.

Since a balanced gain and loss is not always desirable, it is of significant interest to explore EPs in open photonic systems without material loss and artificial gain. Due to the possible radiation losses, EVPs for open systems are non-Hermitian and can have EPs [19–24]. For Maxwell’s equations, the standard EVP formulation regards the frequency ω as the eigenvalue. For open systems, the solutions of the Maxwell EVP are resonant states (also called resonant modes or quasi-normal modes) with complex frequencies [25–30]. A second order EP of resonant states corresponds to the simultaneous coalescence of two complex eigenfrequencies and the corresponding eigenfunctions, and typically requires the tuning of two real

parameters. Therefore, second order EPs are isolated points in the plane of two real parameters. On bi-periodic structures such as photonic crystal slabs, EPs are relatively easy to find, since the resonant states are Bloch waves and the two components of the Bloch wavevector serve as parameters [19, 20]. For two-dimensional (2D) structures that are invariant in one spatial direction and periodic in another, second order EPs of resonant states (in E or H polarization) can be found by tuning one structural parameter and the Bloch wavenumber [23].

Finding a few isolated EPs in a plane of two parameters is relatively easy, but it is difficult to ensure that all EPs in a given domain of parameter space are determined. Moreover, for realizing potential applications, it is highly desirable to understand how EPs depend on parameters of the structure. One approach is to introduce an additional parameter that simplifies the structure in a proper limit, follow the EPs to the limit, and find and analyze the limiting structure. In Ref. [23], we studied EPs of resonant states for a periodic slab with two rectangular segments in each period, followed the EPs as the thickness of the one segment tends to zero, and classifies EPs as connected sets in parameter space indexed by an integer pair (m, n) . However, when the width of the one segment is very small, it is difficult to obtain accurate numerical solutions, because the related linear systems become ill-conditioned. Consequently, we were not able to determine a precise condition for the limiting structure.

In this paper, we consider a slab with a periodic array of circular cylinders, and follow the EPs as the refractive index of the cylinders tends to that of the slab. A numerical method is proposed to study the eigenmodes and EPs of the periodic structure, and it remains well-conditioned even when the refractive indices of the cylinders and the slab are nearly equal. The high accuracy numerical solutions reveal an interesting transition from second order

* Corresponding author: mabdrabou2-c@my.cityu.edu.hk

to third order EPs via a fourth order EP, and allows us to find a precise condition for the limiting uniform slab.

The rest of this paper is organized as follows. In Sec. II, we compare the band structures of a uniform slab and a periodic slab, discuss different kind of eigenmodes and the so-called intrinsic EPs. In Sec. III, we present a track of EPs as a periodic slab approaches its uniform limit, and show the different types of EPs on the track. In Sec. IV, we analyze the limiting uniform slab, and show additional tracks of EPs. The paper is concluded with some remarks in Sec. V.

II. BAND STRUCTURES OF UNIFORM AND PERIODIC SLABS

In Fig. 1(a), we show a periodic array of circular cylin-

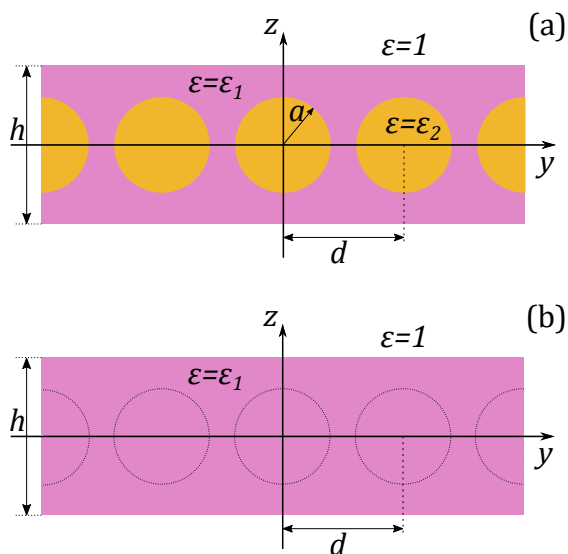


FIG. 1. (a) A dielectric slab with a periodic array of circular cylinders. (b) A uniform slab with a fictitious period.

ders with radius a and dielectric constant ε_2 embedded in a slab with dielectric constant ε_1 . The structure has a period d and a thickness h , and is surrounded by vacuum. A Cartesian coordinate system is chosen such that the structure is invariant in x , periodic in y , and symmetric in z . The dielectric function satisfies $\varepsilon(y, z) = 1$ for $|z| > h/2$. A uniform slab with the same dielectric constant ε_1 and thickness h is shown in Fig. 1(b). We are interested in EPs of resonant states for this periodic slab, especially when $\varepsilon_2 \rightarrow \varepsilon_1$. For the purpose of comparison, the uniform slab is also regarded as a periodic structure with a fictitious period d .

For simplicity, we consider only the E -polarization for which the x -component of the electric field (denoted as u) satisfies the following 2D Helmholtz equation

$$\partial_y^2 u + \partial_z^2 u + k^2 \varepsilon(y, z) u = 0, \quad (1)$$

where $k = \omega/c$ is the freespace wavenumber, ω is the angular frequency, c is the speed of light in vacuum, and

the time dependence is $\exp(-i\omega t)$. A Bloch mode on the periodic slab is a solution of Eq. (1) given as

$$u(y, z) = \phi(y, z) e^{i\beta y}, \quad (2)$$

where $\phi(y, z)$ is periodic in y with period d and β is the Bloch wavenumber. If u decays exponentially to zero as $z \rightarrow \pm\infty$, the Bloch mode is a guided mode. If power is radiated to infinity, i.e., u satisfies outgoing radiation conditions as $z \rightarrow \pm\infty$, then the Bloch mode is a resonant state. We consider only dielectric structures with a real ε , i.e., no material loss or gain. In that case, a guided mode has a real ω and a real β , a resonant state has a real ω and a complex ω with a negative imaginary part.

Corresponding to each Bloch mode $\{u, k, \beta\}$, there is a reciprocal mode at the same frequency for Bloch wavenumber $-\beta$ and a field distribution $v(y, z)$. Since the structure is symmetric in y , we can assume $v(y, z) = u(-y, z)$. If $\{u, k, \beta\}$ is a resonant state with a real β and $\{v, k, -\beta\}$ is its reciprocal mode, then the complex conjugate of v , denoted as \bar{v} , satisfies the Helmholtz equation with k replaced by \bar{k} . In addition, \bar{v} satisfies an incoming wave condition at infinity (the opposite of the outgoing radiation condition), and the associated Bloch wavenumber is β . As in [30], we call this solution $\{\bar{v}, \bar{k}, \beta\}$, the time reversal of the resonant state $\{u, k, \beta\}$. Therefore, a resonant state and its time reversal always appear together for the same β and for k and \bar{k} , respectively.

In addition to the guided modes, Eq. (1) has solutions with real β and real k that grow exponentially as $z \rightarrow \pm\infty$ [31, 32]. These so-called improper modes are not physical if they are considered for all $z \in (-\infty, \infty)$, but on any bounded interval of z , they may be realized as the field profiles of guided modes for some more complicated waveguides with additional high-index structures at larger values of z . Importantly, the improper modes appear when resonant states reach their endpoints as β is increased [30].

In Figs. 2(a) and 2(b), we show the partial band structures of a periodic slab with $\varepsilon_1 = 11.56$, $\varepsilon_2 = 11.50$, $a = 0.25d$ and $h = 1.6d$, and a uniform slab with the same ε_1 and h , respectively. For both cases, only a few odd modes (odd in z) are shown, and for resonant states, only the real part of k is shown. In Fig. 2(b) for the uniform slab, the dashed line is the light line $k = \beta$, the green curves represent guided modes that start from points on the light line, the red curves are folded bands for guided modes with negative propagation constants given by $\hat{\beta} = \beta - 2\pi/d$, the black curves represent resonant states (and their time reversals) with endpoints (purple points) below the light line (visible in the inset), and the blue curves represent improper modes that diverge as $z \rightarrow \pm\infty$ [30–32]. A purple point is a branching point between a pair of resonant state and its time reversal and a pair of improper modes. As shown in the inset, the upper branch of the improper modes converges to the light line at the same point where a band of guided modes is formed. These purple points can be identified as EPs in a non-Hermitian EVP formulation consistent

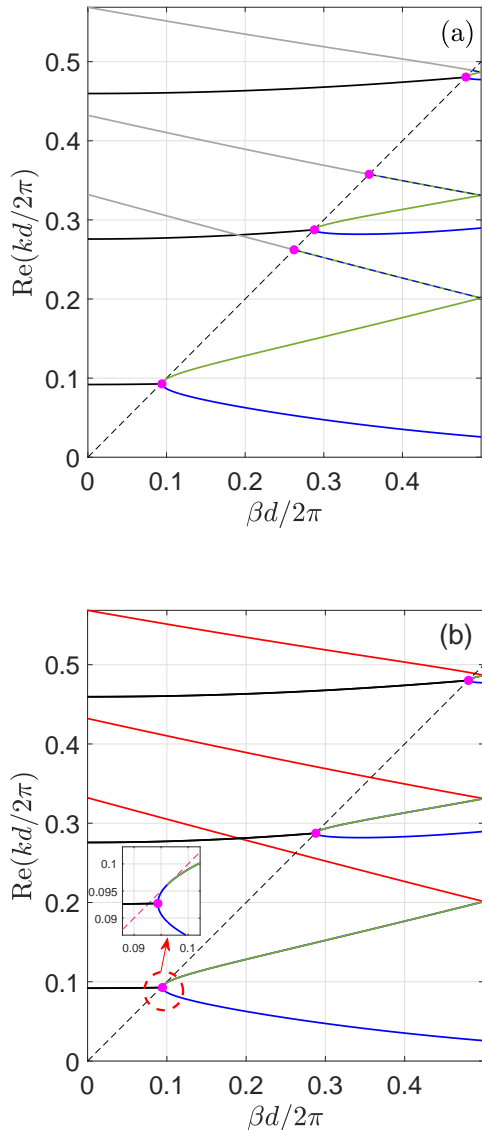


FIG. 2. Band structures for odd modes of a periodic slab (a) and a uniform slab (b). Guided, resonant and improper modes are shown as green, black (or gray) and blue curves, respectively. Folded bands of guided modes are shown as red curves. The purple points are intrinsic EPs.

with resonant states, their time reversals, and improper modes. Since they always exist at the endpoints of dispersion curves for resonant states, we call them intrinsic EPs, and denote them as

$$\text{EP}^{(i)} : (R, \bar{R}) | (I_1, I_2),$$

where R , \bar{R} and I_1 and I_2 signify a resonant state, its time reversal, and two improper modes, respectively. More details can be found in Ref. [30].

Since ε_2 is close to ε_1 , the periodic slab may be regarded as a perturbation of the uniform slab. The solid

green, black and blue curves in Fig. 2(a) are very close to those in Fig. 2(b). Thus, the corresponding guided, resonant and improper modes of the periodic slab are near those of the uniform slab. On the other hand, a folded band of the uniform slab, corresponding to a red curve in Fig. 2(b), is turned to a set containing resonant, guided and improper modes shown as solid gray, dashed green and dashed blue curves in Fig. 2(a). The dashed green and blue curves nearly coincide and are not distinguishable in the figure. The set also contains an intrinsic EP (a purple point) separating the resonant states and improper modes. It is below (but very close to) the light line. Furthermore, a crossing between a black and a gray curve can be observed in Fig. 2(a). At this point, the complex frequencies of the two resonant states have the same real parts, but their imaginary parts are still different. Such a crossing point can be used as a starting point for searching EPs of resonant states.

III. A TRACK OF EXCEPTIONAL POINTS

We are mainly interested in EPs of resonant states at which two or more resonant states coalesce. Typically, a periodic slab with fixed parameters $\{\varepsilon_1, \varepsilon_2, d, a, h\}$ does not have such EPs. A second order EP of resonant states is a codimension-two object corresponding to a point in the plane of two generic real parameters. Therefore, to find a second order EP, we need to tune two parameters. Since resonant states form bands that depend on β continuously, the Bloch wavenumber β can be considered as one parameter. We choose the thickness h of the slab as the other parameter. Therefore, if ε_1 , ε_2 , d and a are fixed, we expect to find second order EPs of resonant states as isolated points in the βh plane. In order to find EPs systematically and understand their dependence on parameters, we vary ε_2 continuously and consider the limit as $\varepsilon_2 \rightarrow \varepsilon_1$. The limit is chosen, because we expect the conditions for the existence of EPs can be simplified as the periodic slab approaches a uniform one.

Using the numerical method described in Appendix, we calculate EPs for a periodic slab with $\varepsilon_1 = 11.56$, $a = 0.25d$, and a varying ε_2 from 9.5 to ε_1 . For each ε_2 , we determine the thickness of the slab, denoted as h_* , so that structure has an EP, and denote the Bloch wavenumber and freespace wavenumber of the corresponding eigenmode by β_* and k_* , respectively. Multiple solutions exist. We call each continuous family of EPs and associated parameters a track. One particular track is shown in Fig. 3(a) for h_* as a function of ε_2 , and in Figs. 3(b) and 3(c) for k_* as a complex-valued function of β_* . Of course, both β_* and k_* depend on ε_2 , but it is more useful to show k_* as a function of β_* . It should be emphasized that the curves in Figs. 3(b) and 3(c) are not dispersion curves of a fixed periodic structure. Each point on these curves corresponds to a distinct periodic slab with a unique value of h_* .

The track consists of two parts separated by point C

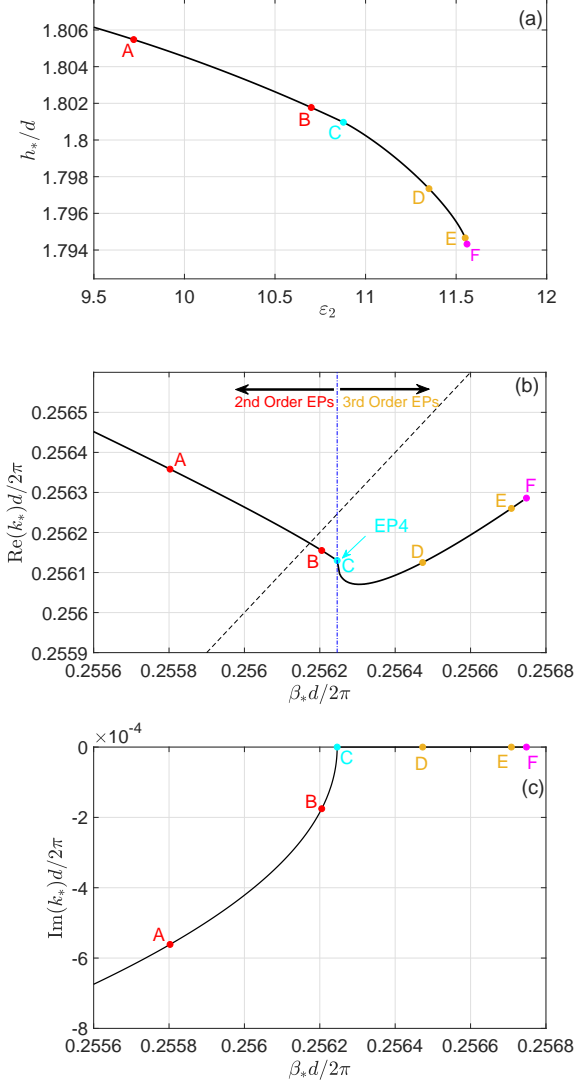


FIG. 3. A track of EPs for a periodic slab with an array of cylinders. (a) Slab thickness h_* vs. ϵ_2 ; (b,c) Trajectories of k_* and β_* as ϵ_2 varies from 9.5 to $\epsilon_1 = 11.56$. A and B are second order EPs of resonant states. D and E are third order EPs with real frequencies. C is a fourth order EP with a real frequency. F is the endpoint of the track.

and ends at point F corresponding to $\epsilon_2 = \epsilon_1$. The EPs on the first part of the track (for smaller values of ϵ_2 , before point C) are second order EPs of resonant states. We denote such an EP by

$$\text{EP2} : (R_1, R_2) | (R_1, R_2)$$

where R_1 and R_2 signify two resonant states. The second part of the track (between C and F) represents third order EPs at which three eigenmodes coalesce at a real frequency. The transition point C is a fourth order EP with a real k_* , and the endpoint F is an intrinsic EP satisfying one additional condition.

On the first part of the track, we choose two points A

and B and show local band structures of the periodic slab at the associated parameter values. Point A corresponds to a periodic slab with $\epsilon_2 = 9.72$ and $h_* = 1.805476d$, and a degenerate resonant state with $\beta_*d = 1.607256$ and $k_*d = 1.610746 - 0.003526i$. In Fig. 4, we show

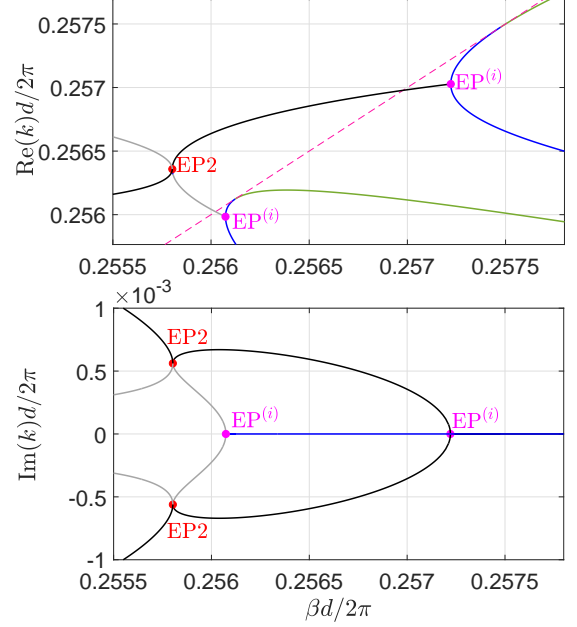


FIG. 4. Local band structure of a periodic slab with the structural parameters of point A. Point A is marked as EP2.

some dispersion curves near this degenerate resonant state marked as EP2. The real and imaginary parts of k are shown in the upper and lower panels, respectively. It is clear that two resonant states, shown as black and gray curves, collapse at the EP with standard square-root splittings for both the real and imaginary parts of k and on both sides of β_* . For $\beta > \beta_*$, the resonant states exist continuously until they reach their ends below the light line at the intrinsic EPs, marked as EP⁽ⁱ⁾ in the figure. The lower panel of Fig. 4 show imaginary parts of both k and \bar{k} corresponding to the resonant states and their time reversals. The EP in the upper half plane, also marked as EP2, is the one for the time reversals.

Point B corresponds to a periodic slab with $\epsilon_2 = 10.70$ and $h_* = 1.801773d$, and a degenerate resonant state with $\beta_*d = 1.609784$ and $k_*d = 1.609470 - 0.001102i$. The local band structure for this periodic slab is shown in Fig. 5. The resonant state for this EP (marked as EP2 in Fig. 5) is below the light line, and is very close to one intrinsic EP. In the lower panel of Fig. 5, both k and \bar{k} are shown. It can be seen that the EP of the resonant states and the EP of the time reversals are very close to each other.

Point C is a fourth order EP obtained when two second order EPs (for the resonant states and their time reversals, respectively) collapse with the nearby intrinsic EP. It corresponds to a periodic slab with $\epsilon_2 \approx 10.877538$

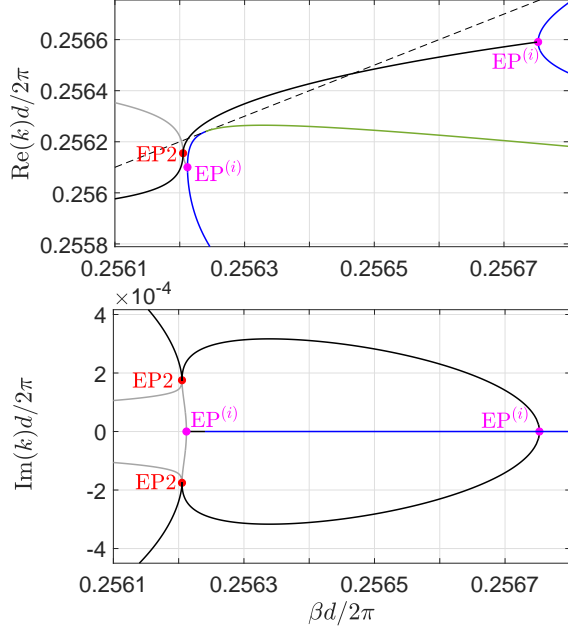


FIG. 5. Local band structure of a periodic slab with the structural parameters of point B. Point B is marked as EP2.

and $h_* = 1.8009676d$, and a degenerate eigenmode with $\beta_*d = 1.6100415d$ and $k_*d = 1.6093126$. It is a fourth order EP, since four modes coalesce at this point. The four modes are two resonant states and their time reversals for $\beta < \beta_*$, and one resonant state, its time reversal, and two improper modes for $\beta > \beta_*$. We denote this fourth order EP as

$$\text{EP4} : (R_1, R_2, \bar{R}_1, \bar{R}_2) | (R, \bar{R}, I_1, I_2)$$

In Fig. 6, we show the band structure for the periodic slab with ε_2 and h_* given above. The resonant states and their time reversals are shown as solid black or gray curves, and the improper modes are shown as solid blue curves. For $\beta > \beta_*$, there is still one resonant mode and its time reversal, and they exist until they reach an intrinsic EP. Moreover, the upper branch of improper modes approaches the light line and ends at the same point where a branch of guided modes emerges.

As ε_2 is further increased, an intrinsic EP appears near the light line. As usual, it connects a resonant state and its time reversal (for smaller values of β) with two improper modes (for larger values of β). One improper mode can collapse with another resonant state and its time reversal to form a third order EP. It turns out that as β passes through its value at this third order EP, there are still a resonant state, its time reversal and an improper mode. Therefore, we denote this third order EP by

$$\text{EP3} : (R, \bar{R}, I) | (R, \bar{R}, I).$$

As an example, we consider point D which corresponds to a periodic slab with $\varepsilon_2 = 11.35$ and $h_* = 1.7973466d$,

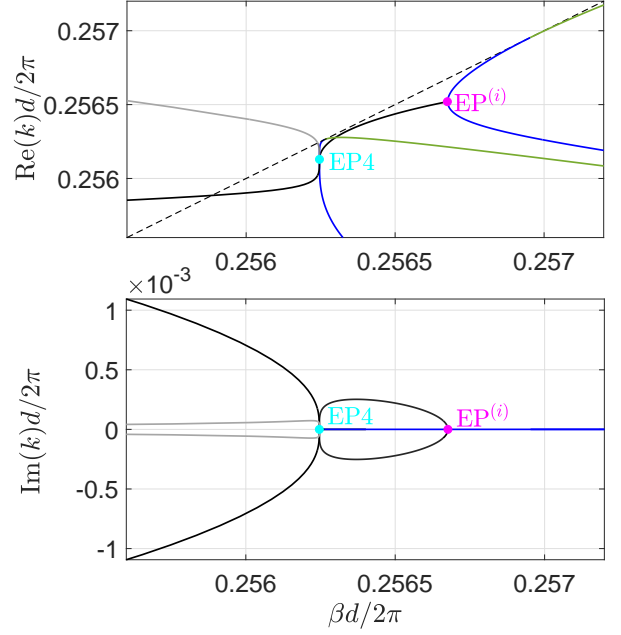


FIG. 6. Local band structure of a periodic slab with the structural parameters of point C. Point C is marked as EP4.

and a triply degenerate eigenmode with $\beta_*d = 1.6114666$ and $k_*d = 1.6092809$. The local band structure of the periodic slab is shown in Fig. 7. We observe that this

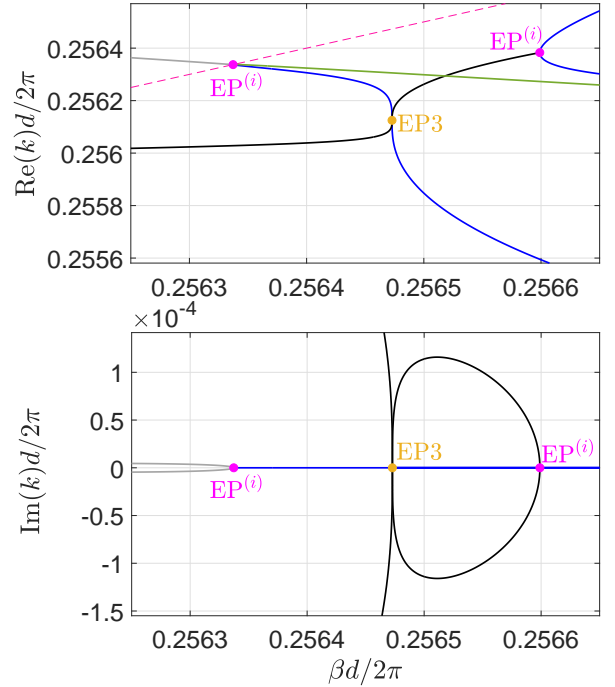


FIG. 7. Local band structure of a periodic slab with the structural parameters of point D. Point D is marked as EP3.

third order EP is connected with an intrinsic EP (at a smaller value of β) by a branch of improper modes, and is connected to another intrinsic EP (at a larger value of β) by a branch of resonant states (and their time reversals).

Point E is another third order EP corresponding to a periodic slab with $\varepsilon_2 = 11.55$ and $h_* = 1.7946619d$, and a degenerate eigenmode with $\beta_*d = 1.6129455$ and $k_*d = 1.61013$. The local band structure of this periodic slab is shown in Fig. 8. We can see that the third order

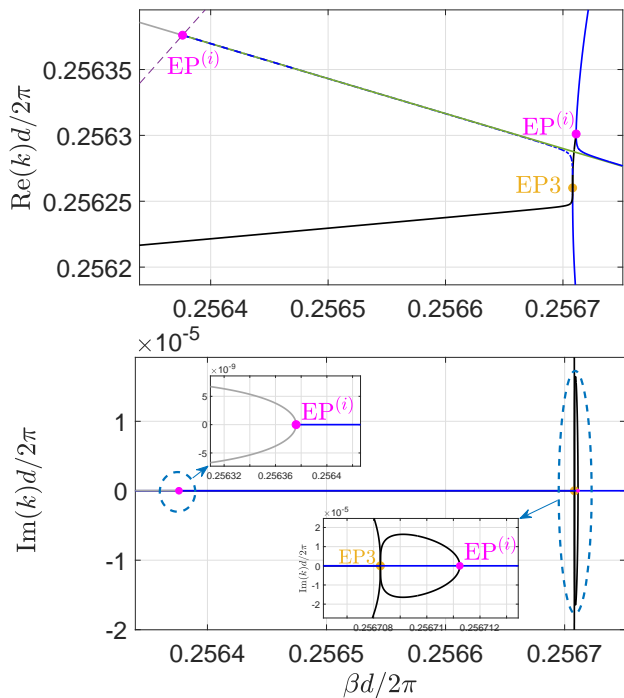


FIG. 8. Local band structure of a periodic slab with the structural parameters of point E. Point E is marked as EP3.

EP is very close to an intrinsic EP that exists at a slightly larger value of β . There is a very short branch of resonant states connecting the third order EP with this intrinsic EP. Another intrinsic EP can be found near the light line. It is connected with the third order EP by a branch of improper modes that nearly coincide with a branch of guided modes.

The final point F is obtained when the third order EP and the intrinsic EP at a slightly larger value of β shown in Fig. 8, merge together as $\varepsilon_2 \rightarrow \varepsilon_1$. It corresponds to a uniform slab with $h_* = 1.7943252d$ and a degenerate eigenmode with $\beta_*d = 1.613197$ and $k_*d = 1.6102917$. As ε_2 tends to ε_1 , the branch of improper modes connecting the intrinsic EP near the light line and the third order EP as shown in Fig. 8, collapses with a branch of guided modes, a new intrinsic EP is formed connecting a branch of resonant states and their time reversals on one side with the two remaining branches of improper modes on the other side. As shown in Fig. 9, point F corresponds to a uniform slab where a folded band of guided

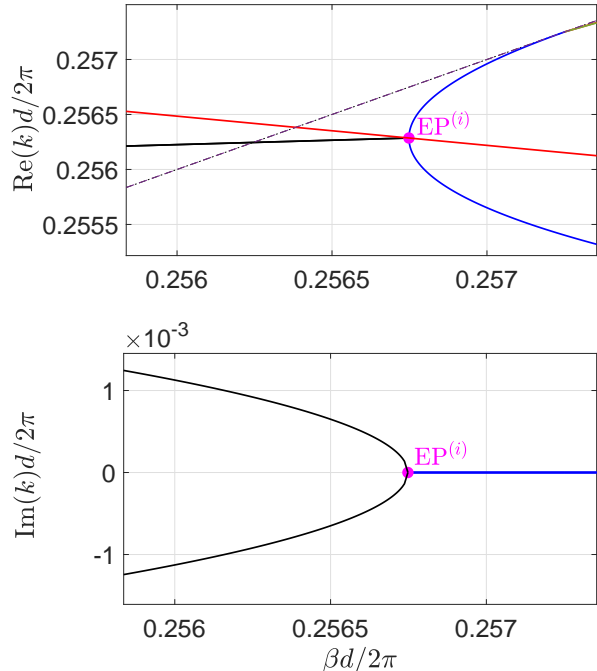


FIG. 9. Local band structure of a uniform slab with the structural parameters of point F. A folded band of guided modes is shown as the red curve. Point F coincides with the intrinsic EP marked as $EP^{(i)}$.

modes intersects with an intrinsic EP.

IV. LIMITING POINTS AND ADDITIONAL TRACKS

Numerical results of the previous section suggest that EPs follow a track with a limiting point corresponding to a uniform slab with a folded band of guided modes intersecting an intrinsic EP. In this section, we analyze uniform slabs satisfying this condition and verify that they indeed give rise to tracks of EPs.

For a uniform slab with dielectric constant ε_1 and thickness h , a guided mode is $u(y, z) = \hat{\phi}(z) \exp(i\hat{\beta}y)$, where $\hat{\beta}$ is the propagation constant and $\hat{\phi}$ tends to zero as $z \rightarrow \pm\infty$. With a fictitious period d in the y direction, the mode can be written as

$$u(y, z) = \phi(y, z)e^{i\beta y}, \quad \phi(y, z) = \hat{\phi}(z)e^{-i2\pi p y/d}$$

for an integer p , such that $\beta = \hat{\beta} + 2\pi p/d \in [-\pi/d, \pi/d]$. A folded band corresponds to a set of modes with a nonzero p and $\beta \in [-\pi/d, \pi/d]$. If $p = 1$, then $\hat{\beta} = \beta - 2\pi/d \in [-3\pi/d, -\pi/d]$.

If the guided mode is odd in z , then

$$\hat{\phi}(z) = \begin{cases} -\exp[\hat{\gamma}_0(z + h/2)], & z < -h/2 \\ \sin(\hat{\gamma}_1 z) / \sin(\hat{\gamma}_1 h/2), & |z| < h/2, \\ \exp[-\hat{\gamma}_0(z - h/2)], & z > h/2, \end{cases}$$

where $\hat{\gamma}_1 = (k^2 \varepsilon_1 - \hat{\beta}^2)^{1/2}$ and $\hat{\gamma}_0 = (\hat{\beta}^2 - k^2)^{1/2}$, and the dispersion curves can be determined from

$$\cot(\hat{\gamma}_1 h/2) + \hat{\gamma}_0 / \hat{\gamma}_1 = 0. \quad (3)$$

The odd guided modes form bands with starting points on the light line given by

$$k = |\hat{\beta}| = \frac{(2n-1)\pi}{h\sqrt{\varepsilon_1 - 1}}, \quad n = 1, 2, \dots$$

The n -th band can be determined from

$$\hat{\gamma}_1 h/2 + \text{arccot}(\hat{\gamma}_0 / \hat{\gamma}_1) = n\pi. \quad (4)$$

An improper mode of the uniform slab is similarly given by $u(y, z) = \phi(z)e^{i\beta y}$, but ϕ grows exponentially as $z \rightarrow \pm\infty$. If the mode is odd in z , then

$$\phi(z) = \begin{cases} -\exp[-\gamma_0(z + h/2)], & z < -h/2 \\ \sin(\gamma_1 z) / \sin(\gamma_1 h/2), & |z| < h/2, \\ \exp[\gamma_0(z - h/2)], & z > h/2, \end{cases}$$

where $\gamma_1 = (k^2 \varepsilon_1 - \beta^2)^{1/2}$ and $\gamma_0 = (\beta^2 - k^2)^{1/2}$. The dispersion relations can be obtained by solving

$$\cot(\gamma_1 h/2) - \gamma_0 / \gamma_1 = 0. \quad (5)$$

The m -th band of improper modes emerges from the same point on the light line as the m -th guided mode, and it can be determined from

$$\gamma_1 h/2 - \text{arccot}(\gamma_0 / \gamma_1) = (m-1)\pi \quad (6)$$

for $m \geq 1$. On each band, β has a minimum which corresponds to an intrinsic EP. Taking the derivative with respect to k for Eq. (5) and setting $d\beta/dk = 0$, we obtain the following condition for intrinsic EPs:

$$\beta^2 = h\varepsilon_1 k^2 \gamma_0 / 2. \quad (7)$$

Therefore, if a folded band of guided modes intersects with an intrinsic EP, we can find h , k and β by solving Eqs. (4), (6) and (7). The band indices must satisfy $m > n \geq 1$.

The case for even modes (even in z) is similar. The n -th guided mode with propagation constant $\hat{\beta}$ and the m -th improper mode with propagation constant β satisfy

$$\hat{\gamma}_1 h/2 - \arctan(\hat{\gamma}_0 / \hat{\gamma}_1) = n\pi, \quad (8)$$

$$\gamma_1 h/2 + \arctan(\gamma_0 / \gamma_1) = m\pi \quad (9)$$

respectively, where $n \geq 0$ and $m \geq 1$. An intrinsic EP corresponds to a minimum of β as a function of k for a

TABLE I. Endpoints for tracks of EPs: uniform slabs with a folded band intersecting an intrinsic EP.

(m, n)	h_*/d	$\beta_* d/2\pi$	$k_* d/2\pi$	parity
(2, 1)	1.794325	0.256748	0.256286	odd
(3, 1)	3.226579	0.238265	0.238112	odd
(3, 2)	2.705984	0.284104	0.283922	odd
(1, 0)	1.273128	0.240640	0.239650	even
(2, 0)	2.658020	0.231293	0.231060	even
(2, 1)	2.265665	0.271347	0.271074	even
(3, 1)	3.752632	0.245890	0.245781	even
(3, 2)	3.124956	0.295280	0.295148	even

band of improper modes. It turns out that the condition $d\beta/dk = 0$ for even improper modes gives the same Eq. (7). Therefore, if a folded band of even guided modes intersects an intrinsic EP, Eqs. (7), (8) and (9) are satisfied.

In Table I, we list a few solutions (denoted as h_* , β_* and k_*) of Eqs. (4), (6) and (7) for odd modes and Eqs. (7), (8) and (9) for even modes, assuming the folded bands are defined by $p = 1$. It is clear that the final point F of previous section corresponds to the case $(m, n) = (2, 1)$ for odd modes. The other solutions also correspond to tracks of EPs. Therefore, we can assign an integer pair (m, n) and parity (odd or even) to each track. In Fig. 10, we show slab thickness h_* as functions

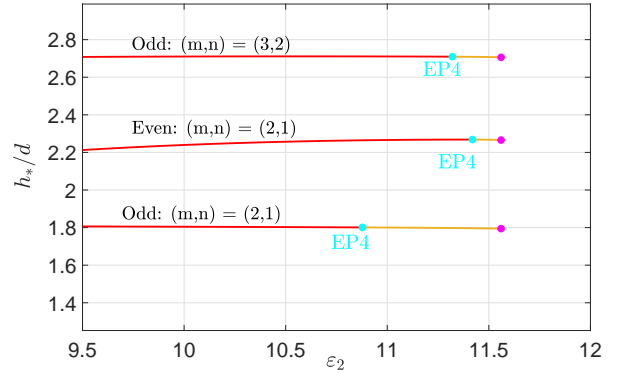


FIG. 10. Three different tracks of EPs for a periodic slab with an array of circular cylinders. The slab thickness h_* is shown as functions of ε_2 .

of ε_2 for three tracks of EPs. The curve marked with “Odd: $(m,n)=(2,1)$ ” is identical to that in Fig. 3(a). All three tracks have the same property. That is, the first part corresponds to second order EPs of resonant states, the second part corresponds to third order EPs, and the transition point is a fourth order EP.

In Ref. [23], we analyzed EPs for a periodic slab with two rectangular segments in each period, and followed EPs as the width of one segment is decreased. Due to numerical difficulties, we only calculated second order EPs of resonant states up to the light line, and obtained an approximate condition for the limiting uniform slab,

namely, a folded band of guided modes intersecting the starting point of guided modes on the light line. For the case of odd modes and $(m, n) = (2, 1)$, the approximate condition gives a slab thickness $h_*^{\text{app}} = 1.801753$, and the relative error $|h_*^{\text{app}} - h_*|/h_*$ is about 0.4%.

V. CONCLUSION

Due to the many interesting properties and potential applications, EPs for photonic structures are being intensively studied by many researchers. Periodic structures have a special advantage related to the degree of freedoms provided by the Bloch wavevector, so that a typical second order EP of resonant states can be found without tuning structural parameters (for bi-periodic structures) or tuning only one structural parameter (for structures with a single periodic direction). In this paper, we analyzed EPs for a dielectric slab containing a periodic array of cylinders. As in our previous work [23], we aim to develop a clear picture about EPs in parameter space by analyzing the limit when the periodic structure approaches a uniform slab. It appears that EPs stay on tracks that can be indexed by a pair of integers and the even/odd parity. The EPs on each track exhibit an interesting transition from second order EPs of resonant states (with complex frequencies) to a special kind of third order EPs with real frequencies, via a fourth order EP also with a real frequency. We also found a precise condition for uniform slabs that correspond to the endpoints of tracks.

Our approach is applicable to more general structures. Instead of calculating isolated EPs by searching parameters locally, we can follow the EPs continuously by tuning parameters towards a simpler structure (such as a uniform slab) and then analyze the simpler structure analytically. For a general 2D periodic structure with a reflection symmetry in z , we expect to obtain the same condition for the limiting uniform slab. If the periodic structure does not have the reflection symmetry in z , the modes can no longer be separated as even and odd ones, a slightly different condition can be expected. Moreover, a similar study can be carried out for bi-periodic structures such as photonic crystal slabs. Our work improves the theoretical understanding on EPs and can provide useful guidance for their practical applications.

ACKNOWLEDGMENTS

The authors acknowledge support from the Research Grants Council of Hong Kong Special Administrative Region, China (Grant No. CityU 11305518).

APPENDIX

To find different kinds of Bloch modes satisfying Eq. (1), we can formulate a linear EVP (for eigenvalue k or k^2) on one period of the structure given by $|y| < d/2$, but it is necessary to truncate z by some technique such as the perfectly matched layer (PML) and discretize the truncated 2D domain. This leads to a linear matrix EVP, but the size of the matrix is relatively large. Alternatively, we can formulate a nonlinear EVP

$$A(\beta, k)w = 0 \quad (10)$$

where the eigenvalue k appears in A implicitly. The advantage of the nonlinear EVP formulation is that A can be approximated by a much smaller matrix and there is no need to truncate z . We use a nonlinear EVP formulation based on a cylindrical wave expansion in the square given by $|y| < d/2$ and $|z| < d/2$, a plane wave expansion in rectangles given by $|y| < d/2$ and $d/2 < |z| < h/2$, and another plane wave expansion in the infinite domains given by $|y| < d/2$ and $|z| > h/2$. For the cylindrical wave expansion, we need to impose the quasi-periodic condition, since u is a Bloch mode given by Eq. (2). The plane wave expansions satisfy the quasi-periodic condition automatically. The system (10) is obtained when the expansions are properly truncated, and continuity conditions are imposed at $z = \pm d/2$ and $z = \pm h/2$. If we consider even and odd modes separately, the size of matrix A can be further reduced. To find the dispersion curves, such as those in Fig. 2(a), we solve k for given β from the condition that A is a singular matrix. Typically, we use the condition $\lambda_1(A) = 0$ where λ_1 is the linear eigenvalue of A with the smallest magnitude.

To find a second order EP of resonant states, we realize that A depends on structural parameters such as the slab thickness h , and solve h , β and k from

$$\lambda_1 = \frac{d\lambda_1}{dk} = 0.$$

A theoretical justification for the second condition $d\lambda_1/dk = 0$ is given in Ref. [24]. Since λ_1 is in general complex, the above two conditions are equivalent to four real conditions. The unknowns h and β are real and k is complex, and thus they are equivalent to four real unknowns. A third order EP in the second part of each track always has a real frequency. We solve real h , β and k from the following three conditions

$$\lambda_1 = \frac{d\lambda_1}{dk} = \frac{d^2\lambda_1}{dk^2} = 0.$$

It turns out that in the regime where such third order EPs exist, λ_1 is always real.

[1] T. Kato, *Perturbation Theory for Linear Operators* (Springer, Berlin, 1966).

[2] W. D. Heiss, "The physics of exceptional points," J. Phys.

- A: Math. Theor. **45**, 444016 (2012).
- [3] M. V. Berry, “Physics of Nonhermitian degeneracies,” *Czech. J. Phys.* **54**, 1039–1047 (2004).
- [4] M.-A. Miri and A. Alù, “Exceptional points in optics and photonics,” *Science* **363**, eaar7709 (2019).
- [5] S. K. Özdemir, S. Rotter, F. Nori, and L. Yang, “Parity-time symmetry and exceptional points in photonics,” *Nature Materials* **18**, 783–798 (2019).
- [6] C. M. Bender and S. Boettcher, “Real spectra in non-Hermitian Hamiltonians having \mathcal{PT} symmetry,” *Phys. Rev. Lett.* **80**, 5243–5246 (1998).
- [7] L. Feng, R. El-Ganainy, and L. Ge, “Non-hermitian photonics based on parity-time symmetry,” *Nat. Photon.* **11**, 752–762 (2017).
- [8] C. E. Rüter, K. G. Makris, R. El-Ganainy, D. N. Christodoulides, M. Segev, and D. Kip, “Observation of parity-time symmetry in optics,” *Nat. Phys.* **6**, 192 (2010).
- [9] B. Peng, Ş. K. Özdemir, S. Rotter, H. Yilmaz, M. Liertzer, F. Monifi, C. M. Bender, F. Nori, and L. Yang, “Loss-induced suppression and revival of lasing,” *Science* **346**, 328–332 (2014).
- [10] M. Brandstetter, M. Liertzer, C. Deutsch, P. Klang, J. Schöberl, H. E. Türeci, G. Strasser, K. Unterrainer, and S. Rotter, “Reversing the pump dependence of a laser at an exceptional point,” *Nat. Commun.* **5**, 4034 (2014).
- [11] L. Feng, Z. J. Wong, R.-M. Ma, Y. Wang, and X. Zhang, “Single-mode laser by parity-time symmetry breaking,” *Science* **346**, 972–975 (2014).
- [12] J. Wiersig, “Enhancing the sensitivity of frequency and energy splitting detection by using exceptional points: application to microcavity sensors for single-part icle detection,” *Phys. Rev. Lett.* **112**, 203901 (2014).
- [13] H. Hodaei, A. U. Hassan, S. Wittek, H. Garcia-Gracia, R. El-Ganainy, D. N. Christodoulides, and M. Khajavikhan, “Enhanced sensitivity at higher-order exceptional points,” *Nature* **548**, 187–191 (2017).
- [14] W. Chen, S. K. Özdemir, G. Zhao, J. Wiersig, and L. Yang, “Exceptional points enhance sensing in an optical microcavity,” *Nature* **548**, 192–196 (2017).
- [15] W. Langbein, “No exceptional precision of exceptional-point sensors,” *Phys. Rev. A* **98**, 023805 (2018).
- [16] M. Zhang, W. Sweeney, C. W. Hsu, L. Yang, A. D. Stone, and L. Jiang, “Quantum noise theory of exceptional point amplifying sensors,” *Phys. Rev. Lett.* **123**, 180501 (2019).
- [17] J. Doppler, A. A. Mailybaev, J. Böhm, U. Kuhl, A. Girschik, F. Libisch, T. J. Milburn, P. Rabl, N. Moiseyev, and S. Rotter, “Dynamically encircling an exceptional point for asymmetric mode switching,” *Nature* **537**, 76–79 (2016).
- [18] A. U. Hassan, B. Zhen, M. Soljačić, M. Khajavikhan, and D. N. Christodoulides, “Dynamically encircling exceptional points: exact evolution and polarization state conversion,” *Phys. Rev. Lett.* **118**, 093002 (2017).
- [19] B. Zhen, C. W. Hsu, Y. Igarashi, L. Lu, I. Kaminer, A. Pick, S.-L. Chua, J. D. Joannopoulos, and M. Soljačić, “Spawning rings of exceptional points out of Dirac cones,” *Nature* **525**, 35 (2015).
- [20] P. M. Kamiński, A. Taghizadeh, O. Breinbjerg, J. Mørk, and S. Arslanagić, “Control of exceptional points in photonic crystal slabs,” *Opt. Lett.* **42**, 2866–2869 (2017).
- [21] H. Zhou, C. Peng, Y. Yoon, C. W. Hsu, K. A. Nelson, L. Fu, J. D. Joannopoulos, M. Soljačić, and B. Zhen, “Observation of bulk Fermi arc and polarization half charge from paired exceptional points,” *Science* **359**, 1009–1012 (2018).
- [22] J. Kullig, C.-H. Yi, M. Hentschel, and J. Wiersig, “Exceptional points of third-order in a layered optical microdisk cavity,” *New. J. Phys.* **20**, 083016 (2018).
- [23] A. Abdrabou and Y. Y. Lu, “Exceptional points of resonant states on a periodic slab,” *Phys. Rev. A* **97**, 063822 (2018).
- [24] A. Abdrabou and Y. Y. Lu, “Exceptional points for resonant states on parallel circular dielectric cylinders,” *J. Opt. Soc. Am. B* **36**, 1659–1667 (2019).
- [25] M. Tsuji, H. Shigesawa, and K. Takiyama, “On the complex resonant frequency of open dielectric resonators,” *IEEE Transactions on Microwave Theory and Techniques* **31**, 392–296 (1983).
- [26] A. W. Glisson, D. Kajfez, and J. James, “Evaluation of modes in dielectric resonators using a surface integral equation formulation,” *IEEE Transactions on Microwave Theory and Techniques* **31**, 1023–1029 (1983).
- [27] S. Fan and J. D. Joannopoulos, “Analysis of guided resonances in photonic crystal slabs,” *Phys. Rev. B* **65**, 235112 (2002).
- [28] D. A. Powell, “Resonant dynamics of arbitrarily shaped meta-atoms,” *Phys. Rev. B* **90**, 075108 (2014).
- [29] W. Yan, R. Feggiani, and P. Lalanne, “Rigorous modal analysis of plasmonic nanoresonators,” *Phys. Rev. B* **97**, 205422 (2018).
- [30] A. Abdrabou and Y. Y. Lu, “Indirect link between resonant and guided modes on uniform and periodic slab,” *Phys. Rev. A* **99**, 063818 (2019).
- [31] S. Yamaguchi, A. Shimojima, and T. Hosono, “Analysis of leaky modes supported by a slab waveguide,” *Electron. Comm. Jpn. Pt. II* **73**, 20–31 (1990).
- [32] G. W. Hanson and A. B. Yakovlev, “An analysis of leaky-wave dispersion phenomena in the vicinity of cutoff using complex frequency plane singularities,” *Radio Sci.* **33**, 803–819 (1998).